Legacy Effects of Forest Clearcutting on Ecosystem Function and Biogeochemical Cycling in a New England Forest

By

Andre S Gomes

An Honors Project submitted in Partial Fulfillment of the Requirements for Honors

in

The Department of Biology

Rhode Island College

2023

Legacy Effects of Forest Clearcutting on Ecosystem Function and Biogeochemical Cycling in a New England Forest

An Undergraduate Project Presented

By

Andre S Gomes

To

The Biology Department

Approved:

_____	_____
Project Advisor Date	Date
_____	_____
Chair, Department Honors Committee Date	Date
_____	_____
Department Chair	Date

Abstract

Terrestrial soils comprise the largest reservoirs of carbon (C) in the biosphere holding some 2500 Gt C, which is 4x the amount found in plant biomass and 3x the C content of the atmospheric pool. Approximately 1500 Gt of soil C is in an organic form, thus making it available to mineralization by heterotrophic organisms. Changes to the drivers of mineralization such as climate change and aeration due to anthropogenic land use, such as logging, have the potential to strongly affect global carbon and associated nutrient cycles, plant production, and atmospheric composition [10]. With the aim of better understanding the potential long-term implications of forest logging on ecosystem function and soil biogeochemistry we conducted a range of measurements in the field and laboratory to elucidate patterns along a 20-year old clearcut and adjacent 100+ year old forest stand located in two experimental large gaps in Yale Myers Forest, Eastford, CT. A decrease in organic matter and reduced soil biotic activity in the experimental large gaps when compared to the 100+ year old forest due to the potential changes in edaphic conditions and biodiversity associated with disturbance is expected. Leaf litter samples collected from the study sites Kozy Road and Tree Heaven underwent elemental analysis to measure the change in litter carbon and nitrogen throughout the experiment. Soil samples were collected at each litterbag collection throughout the sampling period to provide a surface and subsurface snapshot of the biology at that time in each transect. Soil samples were analyzed for four ecoenzymes that play a pivotal role in carbon and nutrient cycling in soil, β-glucosidase (BG), Acid Phosphatase (AP), β-N-acetylglucosaminidase (NAG), and β-Xylosidase (XYLO). Results found an overall increase in average C and N percentages in both Kozy Road and Tree Heaven over the course of this study, which may indicate mineralization and immobilization is occurring and resulting in an accumulation of soil organic matter. The highest EEA values were found for BG and AP. This result may be explained by the fact that BG hydrolyzes cellulose. Acid Phosphatase works upon organic phosphorus and converts it into its inorganic form, an essential nutrient for all life. Labile organic material and organic phosphorus were the primary targets of the ecoenzymes analyzed in this study. In the coming months, we plan to continue to measure and collect data from samples collected beyond the nine month cutoff for this study extending data collection to 12 and 18 months in order to conduct more intensive hypothesis testing and multivariate statistics.

Table of Contents

Chapter I

Climate Change

Predictive Earth System Models estimate that Earth's mean annual atmospheric temperature will increase by 1.1 to 5.4ºC by the year 2100 depending on emissions scenarios of greenhouse gases, which are predominantly a result of fossil fuel combustion and agriculture practice by humans [1]. Greenhouse gases are those that trap solar radiation in the atmosphere, and thus increase the overall temperature of the Earth's atmosphere, and indirectly oceans and terrestrial land surfaces. Greenhouse gases most abundantly associated with human activities include carbon dioxide (CO_2), methane (CH_4), nitrous oxides (NOx), water vapor, and fluorinated synthetic gases [2]. Carbon dioxide is the most abundant GHG that is associated with anthropogenic activity and is considered the basis for quantifying the relative warming effect of other GHGs. For example, the CO_2 equivalence (CO_2e) of CH_4 is 25x-CO_2e, making CH_4 a potent GHG. In addition to having different warming potentials, GHGs have vastly different residence times in the atmosphere, for example CO_2 resides in the atmosphere for 300 to 1000 years, while CH_4 only resides in the atmosphere for 8 years.

Anthropogenic activity including agriculture and fossil fuel combustion has been the primary culprit for the sudden increase in the rate of global climate change since the industrial revolution (1880-1900). The Earth's temperature has increased by an average of 0.08ºC per decade since 1880. In 2022, global surface temperatures were recorded and compared to the pre-industrial period. Surface temperatures have risen 1.06ºC since the pre-industrial period. Since 1981 the rate of warming was calculated to be 0.18ºC per decade and this rate is expected to increase exponetially as GHG emissions and associated positive-feedback loops result in greater emissions. The year 2022 was the 6th warmest year on record based on NOAA temperature data

and the 10 warmest years in the historical record have all occurred since 2010 [3]. In 2020, CO_2 accounted for 79% of all U.S. greenhouse gas emissions [2].

CO_2 occurs naturally in the atmosphere and was long balanced by photosynthesis and cellular respiration in the global carbon cycle. However, by extracting and burning fossil fuels, humans have perturbed the natural balance of the global ecosystem by injecting long sequestered GHGs into the atmosphere. Leading fossil fuels such as coal, natural gas and oil for energy and transportation accounts for approximately 64% of CO_2 emissions in the U.S. in 2020. Industrial, residential, commercial, and other non-fossil fuel combustion activities accounted for the remaining 36% [2]. Anthropogenic activities that influence CO_2 concentrations in the Earth's atmosphere are not solely limited to fossil fuel combustion. The clearing of vast grasslands for agriculture has also negatively affected plant and soil biotic communities, by disrupting both their ability to capture and store carbon, and ultimately carbon from the atmosphere in the form of soil organic carbon (SOC). Tilling land for cultivation also releases vast amounts of long sequestered soil organic carbon that originated as plant roots, organic compounds (e.g., root exudates) and organic matter that was partially decomposed by soil biotic communities (e.g., humus). This release of GHGs as a result of soil aeration leads to a positive feedback that increases GHGs and atmospheric temperature, which in turn enhances soil respiration rates due to warming conditions. Another anthropogenic activity that has increased CO_2 emissions is the depletion of large herds of animals that once grazed vast stretches of land around the globe leading to the evolution of vast native grassland communities. Large herds were responsible for the trampling of dead vegetation and aided in their decomposition and the association of organic matter into soils (i.e., SOM stabilization), as well as depositing manure possibly containing seeds, and nutrients that fertilize plant communities. In addition to tillage, clearing forests (i.e.,

timber harvest) and other natural ecosystems to access natural resources or create space for agriculture, urban development, roadways, and other resource driven endeavors, have all contributed to an increase in CO_2 emissions, disrupted the natural balance of carbon fixation and respiration, and ultimately decreased the natural ability of ecosystems to sequester carbon from the atmosphere. Since the advent of mechanized equipment for agriculture during the Industrial Revolution, agricultural land practices have accounted for the release of 50-100 GT of C from the soil to the atmosphere, exacerbating positive feedbacks to climate change [4].

An increase in mean annual global temperatures due to increased concentrations of CO_2 in the atmosphere will alter the natural biogeochemical cycles that have evolved along with, and as a part of, Earth's biotic communities. These cycles are inherent to the regulation of global climate and other life sustaining services such as the global water cycle. As temperatures rise plant, animal, and microbial community level adaptations such as shifts in aspects of life cycles, phenology, and ecophysiology (e.g., enzymatic activities associated with metabolic processes) to survive in changing habitat conditions. The potential challenges communities face include displacement, migration and potentially extinction if climate change effects outpace adaptation. These outcomes would only further increase CO_2 emissions through increased decomposition, soil respiration, and loss of ecosystem goods and services that all living organisms on Earth rely upon.

Chapter II

Carbon Cycle

Carbon (C), nitrogen (N) and phosphorus (P) are critical elements that are necessary for life [6]. The biogeochemical cycles that regulate the stoichiometry of ecosystems have been widely studied and documented [10]. The cycles of C and oxygen are inexorably linked as they are seen bonded or balanced in all ecosystems and the majority of life forms. The carbon cycle is a crucial life sustaining biogeochemical cycle in which carbon is exchanged through the biosphere, lithosphere, oceans, and the atmosphere [5].

In the atmosphere C exists most abundantly as CO_2. Variations in the atmospheric concentrations of CO_2 are driven by seasonal uptake of CO_2 by photosynthesis particularly in the northern hemisphere, seasonal differences in the use of fossil fuels, and the exchange of CO_2 between the atmosphere and the oceans [6]. As discussed in the previous section, climate, CO_2, and CH_4 are considered greenhouse gases and their relative atmospheric concentrations are a main driver of climate change. Greenhouse gases regulate global temperatures and allow solar energy to be trapped in the atmosphere in the form of heat. These gases were an integral component that were responsible for the warming of the planet, and they have allowed liquid water and life to flourish on Earth. However, the sudden and exponential increase in global temperatures since the Industrial Revolution is due to anthropogenic causes, mainly the burning of fossil fuels. The rate at which CO_2 is released into the atmosphere through the burning of fossil fuels, relative to the rate at which the oceans can uptake C, accounts for the precipitous increase of atmospheric CO_2 we see today [6].

The anthropogenic burning of fossil fuels since the Industrial Revolution has added a novel element to the C cycle in modern times. Combusting fossil fuels such as coal, natural gas and oil for energy and transportation has dramatically increased atmospheric CO_2 concentrations. The U.S., China, and India are the largest generators of anthropogenic CO_2 emissions in the

world; 10,065 Mt, 5,416 Mt, 2,654 Mt of CO_2 released respectively in 2019 [7]. The amount of CO_2 being released into the atmosphere is shifting the balance of the natural carbon cycle, such that the rate of photosynthesis is being outpaced by GHG emissions and biotic respiration. If strategies to mitigate this modern phenomena are not deployed (e.g., reductions in GHG emissions), global temperatures will continue to increase and affect Earth's climate system. A rise in global temperatures would stand to threaten much of the planet's existing biodiversity through a myriad number of disturbances.

Carbon is found in all living organisms and is the backbone of all organic molecules (e.g., carbohydrates, proteins, lipids). Carbon may exist in different forms and states depending on where it is found in the C cycle. Living organisms utilize C for their cellular structures and release it in the form of CO_2 as a product of respiration. Carbon is also found in the lithosphere, the rigid outermost rocky shell of the planet [5]. Sedimentary rocks in the lithosphere contain vast stores of C in the form of fossilized dead organic matter. These vast stores of fossilized material, or fossil fuels, are mined by humanity and burned for energy. When combusted, fossil fuels release large quantities of C in the form of CO_2 back into the atmosphere [6].

Another reservoir for C in the lithosphere is SOC which can be found in the uppermost layer of the earth's crust and accounts for the largest terrestrial carbon sinks. The total C found in terrestrial ecosystems is approximately 3,170 Gt. Soils contain approximately 80% of terrestrial C stores, 2,500 Gt. The soil carbon pool is second only to the oceans [4]. The main avenue for the transfer of C (CO_2) from the atmosphere to the lithosphere is by the process of photosynthesis by land plants. Plants fix CO_2 from the atmosphere by reducing it and converting it into organic carbon. Organic C is utilized in the production of biomass and this process is directly tied to net primary production in land plants. Plant biomass and rates of growth in turn

affect the composition of the atmosphere. Organic C that can be found in the soil originates from dead plants, animals and other living organisms which have been decomposed. Inorganic C may also be found in the soil and is a result of the weathering of mineral rocks and the biologically mediated mineralization of calcium carbonate in arid and semiarid regions resulting in the formation of petrocalcic soil horizons also known as caliche [8,9]. The accumulation and turnover rate of C in the soil is dependent on environmental factors, mainly precipitation and temperature levels, and decomposition rates that are driven by temperature, soil moisture, litter quality, and decomposer organisms. However, SOC exists in a small fraction of the overall soil and can be highly variable globally and sensitive to climate change. The maintenance of forest ecosystems, proper land use, sustainable agriculture and deforestation are all of vital importance when considering atmospheric concentrations of CO_2 and terrestrial carbon sequestration; and consequently, climate change. Two-thirds of the total exponential increase in atmospheric CO_2 concentrations in modern times is due to the burning of fossil fuels, while the remainder is attributed to SOC loss due to land use change [4]. Areas considered net C sinks are crucial ecosystems that mitigate the effects of climate change.

Chapter III

Decomposition & Extracellular Enzymes

Terrestrial soils comprise the largest reservoirs of carbon (C) in the biosphere holding some 2500 Gt C, which is 4x the amount found in plant biomass and 3x the C content of the atmospheric pool. Approximately 1500 Gt of soil C is in an organic form, thus making it available to mineralization by heterotrophic organisms. Changes to the drivers of mineralization such as climate change (i.e., temperature and moisture) and aeration have the potential to strongly affect global carbon and associated nutrient cycles (e.g., organically bound N or P), plant production, and atmospheric composition [10]. Decomposition is one of the most important biological processes given its role in the formation of soil carbon (e.g., humus) and its regulatory role in ecosystem C cycling. Decomposition is a metabolic process in which dead organic material is transformed by environmental factors and decomposer organisms such as bacteria and fungi. During the decomposition process the bonds between organic polymer molecules are hydrolyzed into their more readily digestible monomer forms. They are then transported and transformed through mineralization by decomposer organisms into inorganic nutrients that can be taken up by plants and animals, thus restarting the cycle. Decomposition rates are affected by climatic variation (e.g., temperature, moisture), edaphic properties (e.g., soil pH and texture), and biotic factors (e.g., litter quality, and decomposer communities). Given the multifactorial nature of this process, it varies widely between different ecosystems. Generally, decomposition rates are faster in warm-wet (e.g., tropical) conditions highlighting the importance of temperature and soil moisture, which is affected by precipitation rates along with soil texture (e.g., clay, sand, and silt content). When temperatures are extremely high soil moisture will decrease due to evaporation and in turn decomposition rates will be low. Conversely, very low temperatures will also have a negative impact on soil moisture levels and decomposer organism activity. Biotic factors such as decomposer organisms may experience shifts in their metabolic rates, biomass, community

compositions, and consequently overall decomposition rates and nutrient input into soils due to climate change [11]. The decomposition process is sequential and divided into phases characterized by the litter compounds that are being broken down. Early on, detritus is colonized by fast-growing, opportunistic microorganisms with high affinities for soluble, labile, substrates. Then, these organisms are succeeded by slower growing decomposers that specialize in holocellulose degradation. Lastly, after all non-lignified polysaccharides are consumed, oxidative breakdown of lignin and humic condensates, recalcitrant carbon molecules, begins and is performed by slow-growing decomposers [12]. Material that is not decomposed may become occluded in mineral soil and integrate into soil organic matter for years to decades, and in poorly aerated or cold soils for centuries and beyond. Labile soil carbon mainly consists of soil microbial biomass carbon, dissolved organic matter, and easily oxidative organic matter whereas recalcitrant soil carbon is resistant to microbial decomposition or is protected by mineral soil particles (e.g., lignin) [13]. Decomposer organisms consist of microfauna to megafauna and are classified based on body size. Microfauna such as bacteria and fungi are some of the most essential decomposers of dead organic matter in soil and are greatly affected by changes in temperature, pH, and moisture content.

Extracellular Enzymes: The proximate agents of organic matter decomposition

Microorganisms such as fungi and bacteria (plants as well) excrete specific enzymes into the soil matrix in order to catalyze hydrolysis reactions with complex organic carbon molecule substrates. These enzymes transform available organic matter by mineralization, while liberating inorganic mineralized nutrients that can be taken up by plants and other organisms. Extra cellular enzymes acting in the environment, known as ecoenzymes (EE), are excreted by fungi and

bacteria when substrates are available, and growth is required [12]. Competition from cheaters (microbes that don't produce enzymes but take up products), slow rates of diffusion (due to inadequate moisture levels), and N limitation may limit microbial foraging and the decomposition of complex compounds [14]. EEs are the proximate agents of organic matter decomposition and measures of these activities can be used as indicators of microbial nutrient demand [10]. Microbial nutrient demand may be quantified by comparing elemental stoichiometry of microbial biomass to environmental nutrient availability [15]. EE activity (EEA) links environmental nutrient availability with microbial production, and macroscale patterns in EEA may uncover the limitations on microbial biomass stoichiometry and enzyme relationships to soil organic matter (SOM) composition and the biochemical controls on soil C storage. EEAs catalyze the rate-limiting step in organic matter (OM) degradation and as such, correlations between EEA, plant litter decomposition, and microbial production are linked [10].

Dead plant organic matter such as cellulose and lignin are the most abundant components of plant litter. EE such as β-glucosidase (BG) that catalyze the hydrolysis reaction of cellobiose to glucose are especially of interest, and their activity levels are key indicators of microbial nutrient demand during the decomposition process [15]. β-Xylosidase (Xylo) is an exoglycosidase enzyme that hydrolyzes the non-reducing ends of xylo-oligosaccharides into the more basic form, xylose [16]. Xylose and arabinose are the primary constituents of hemicellulose and are found in agricultural waste such as rice straw, corn cobs and in part of hard wood trees and shrubs [17].

Other important enzymes involved in the decomposition of organic matter in soils hydrolyze chitin. Chitin is the second most abundant natural polysaccharide found in terrestrial

soils after cellulose. Chitin can be found in the exoskeletons of arthropods, shrimps, insects and also in fungi and bacteria [18]. Chitin is degraded by the EE β-N-acetylglucosaminidase (NAG).

Phosphorus is an essential nutrient for plant growth, and all life on the planet. It is mainly formed by the weathering of mineral rock. Its cycle compared to the oxygen, nitrogen, carbon, and hydrogen cycle is very slow and can take millions of years to complete one cycle. Most phosphorus is leached away and ends up in aquatic sediment [19]. The EE Acid Phosphatase (AP) is in a family of enzymes that are ubiquitous in nature and found in animals and plants. It is a hydrolase that catalyzes the hydrolysis of orthophosphate monoesters under acidic conditions into inorganic phosphate; an essential nutrient for plant and animal growth [20].

Together these four EE may provide a comprehensive insight into microbial nutrient demand and thus help provide a link between EEA, SOM, and SOC in terrestrial soils. The measurement of EEA can thus provide quantitative data on the rates of decomposition and nutrient availability in soils. This information is thus key when attempting to quantify the effects of climate change and land use such as agricultural and forestry practices on the largest reservoirs of carbon in the biosphere, terrestrial soils.

Chapter IV

Effects of Anthropogenic Land Use on Soil Organic Matter and Carbon Sequestration

Anthropogenic activities such as urbanization, the clearing of fields for agriculture and development, and selective logging all have the potential to decrease SOC storage and thus hinder the C sequestration abilities inherent in terrestrial forest ecosystems. Photosynthesis fixes and stores C at a rate of approximately 3 GT yr^{-1}. This rate is faster than the rate at which the oceans sequester C from the atmosphere, 2 GT yr^{-1}. Thus, making terrestrial forest ecosystems an integral element in the global carbon cycle and climate change mitigation. The accumulation of organic matter through C fixation and rates of decomposition in forest soils is of vital importance [4].

Organic matter affects the physical, chemical, and biological properties of soil. SOM improves soil quality by increasing water and nutrient retention which results in greater NPP in natural and human-made settings. SOM also improves soil structure which in turn may reduce erosion, nutrient leaching, and lead to an improvement in ground and surface water quality. Proper management, conservation, and restoration practices of SOC and OM levels in forest ecosystems directly impact the exponential increase of CO_2 in the atmosphere, and are primarily driven by rates of photosynthesis, decomposition, and respiration [4].

Approximately 2/3 of the increased concentration of CO_2 in the atmosphere today is due to the burning of fossil fuels, and the rest is due to land use change. Soil disturbances affect soil temperature and moisture levels. Soil characterization and temperature are key mediators of photosynthesis and decomposition. An increase in soil temperature due to gaps created in forest canopies and the clearing of shrubs and slash may lead to increased rates of SOM decomposition and higher microbial activity, while moisture levels remain adequate. Increased rates of SOM decomposition result in increased rates of respiration and released CO_2. This process has the potential to create a positive feedback loop and further the effects of climate change globally [4].

Land use that reduces C inputs or increases C losses compared to natural vegetation results in reductions in SOC over time and create a SOC deficit relative to C levels that existed in the soil before the disturbance [4]. Disturbances are a natural part of ecosystem ecology and occur at different spatial and temporal scales. Disturbances are an essential component of evolution and are considered a major driver of plant ecological strategies, and community assemblage and maintenance [21]. Natural disturbances such as forest fires and the death of one-several trees create canopy gaps and opportunities for young saplings and other forest inhabitants and are the first stage in forest succession. Studies have shown that intermediate levels of disturbance, those that leave behind a patchwork of older stands and do not lose all their soil biota, are the most beneficial to future succession and regeneration. Previous disturbances have been shown to impact the response of plant communities to subsequent disturbances [22].

Forest responses to climate change may be affected by past anthropogenic land use disturbances such as logging. Logged forests show arrested succession as seen by their reduced abundance of biomass-accumulators such as large-seeded pioneer species. Levels of above ground biomass are larger in mature, unlogged forests. Lower levels of functional diversity are also observed in logged forests. Unsustainable selective logging, like clear-cutting (when all tree stands, shrubs and slash are completely removed), can produce enduring functional changes in forest trait distribution, a collapse in logged populations, and arrested succession. Together with climate change, non-sustainable logging practices such as clear cutting may change forest dynamics and functionality. Changes in forest structure, species richness, floristic composition, species ecological strategies, and photosynthetic and decomposition rates are to be expected as a result [22].

Yale Myers Forest Study Sites

Fragmentation creates edges between forested and non-forested areas that have ecological effects on the remaining forest. An estimated 62% of forested lands in the US are located within 150 m of an anthropogenic created forest edge. Forest edges change the microclimate in the surrounding environment and have the potential to limit available resources such as light, soil moisture, and soil nutrients. Furthermore, a change in the soil microclimate may impact local abiotic and biotic constituents that in turn may affect rates of decomposition, SOM accumulation, and SOC sequestration. Forest edges created by anthropogenic gaps due to land use practices may temporarily or permanently change forest community dynamics. Experimental large gaps (ELG) created in terrestrial forest ecosystems are a useful system for research on these matters. ELGs lack the possible confounding factors such as increased air and water pollution, and the existence of exotic plants and animals that are associated with forest edges created by urbanization and agricultural use. As such, ELG provide an optimal setting for forest edge research.

The Yale Myers Forest located in Eastford, Connecticut contains 7800 acres of temperate forest and is owned and managed by the Yale University School of Forestry and Environmental Studies. During the winter of 1999-2000 two ELGs were established, Tree Heaven and Kozy Road, by clear cutting (including all shrubs and slash) 110 m x 25 m areas in Yale Myers Forest for research purposes. The ELGs were allowed to regenerate naturally since the cut. At the time of de Gouvenain et al. study in 2009 vegetation in the gap had an average dbh of < 5 cm and was dominated by < 10-year-old patchy sweet birch [23].

The goal of this study is to better understand the potential long-term implications of forest logging on ecosystem function and soil biogeochemistry. The hypothesis of this honors

thesis is that a decrease in organic matter and reduced soil biotic activity (EEA) in the experimental large gaps when compared to the 100+ year old forest is expected due to the potential changes in edaphic conditions and biodiversity associated with disturbance. Elemental analysis of leaf litter and extracellular enzyme activity analysis of soil may indicate legacy effects from the 20-year old clearcut and into the adjacent 100+ year old forest stand.

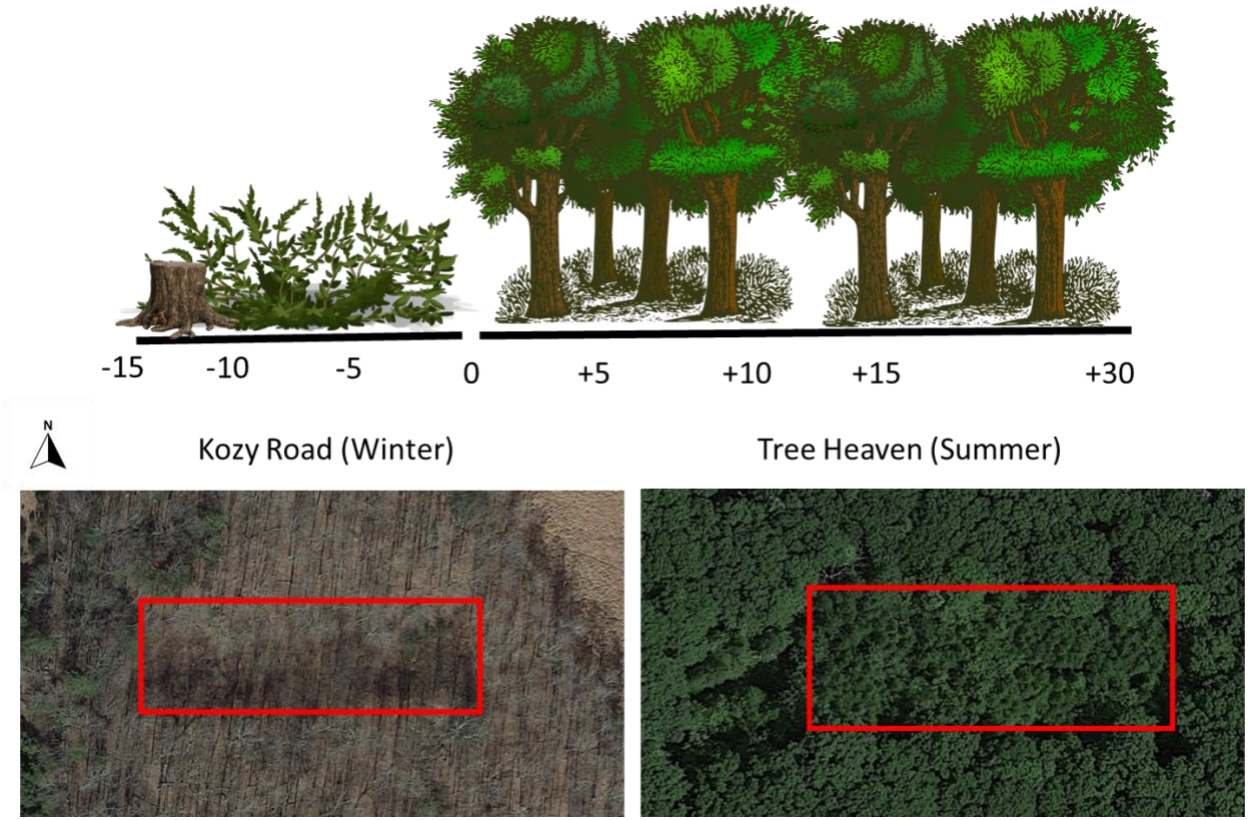

Figure 1. Yale Myers Forest study sites Kozy Road and Tree Heaven. (Top) Illustration of the transect layout for both sites. Distances range from the beginning of the ELG (distance -15 m), to the forest edge (denoted 0 m), and (+30 m) into the old growth forest. (Bottom) Google Maps satellite images of the Yale Myers Forest sites used for this study. Kozy Road: 41.9422, -72.1244 (decimal notation). Tree Heaven: 41.9889, -72.1248 (decimal notation). [Kozy Road] [image retrieved 04/07/2023]. Google Maps. [Tree Heaven] [image retrieved 04/07/2023]. Note seasonal difference in images affect canopy cover.

Materials & Methods

Original Transect Layout by de Gouvenain et al.

In 2009, Dr. Roland de Gouvenain established four 10 m wide by 40 m long belt transects from randomly selected starting points along the northern edge of the Tree Heaven ELG. These transects ran perpendicular to the east-west oriented edge of the ELG. Transects ran from 10 m into the gap to 30 m into the forest, following methods of McDonald and Urban (2004). The mid-line of each transect was located at least 10 m away from any other transect mid-line. The same procedure was used in establishing the transects at Kozy Road during the same time period. In early 2016 de Gouvenain, along with Hewins, extended these transects 10 m further into the gaps [23].

Transect layout expansion and study site selection by Hewins et al.

On the dates of November 4th, 5th, 11th, and 12th in 2016 Hewins et al. established study locations along de Gouvenain's transects at the Tree Heaven and Kozy Road ELG sites. A 0.5 m^2 quadrat frame was constructed out of PVC pipe. Quadrat transects were randomly dropped twice along de Gouvenain's original transects (East-West directionality), once on the Northern and once in the Southern side within the belt transect. These locations were located at 15, 10, and 5 meters into the gap (here after -5, -10 and -15 m), at the exact gap edge (denoted 0), and 5, 10, and 15 meters into the forest (here after +5, +10, +15 and +30) following along de Gouvenain's original transect layout approximately. These study locations would serve as the site of soil sampling and leaf litter sampling and decomposition experiments.

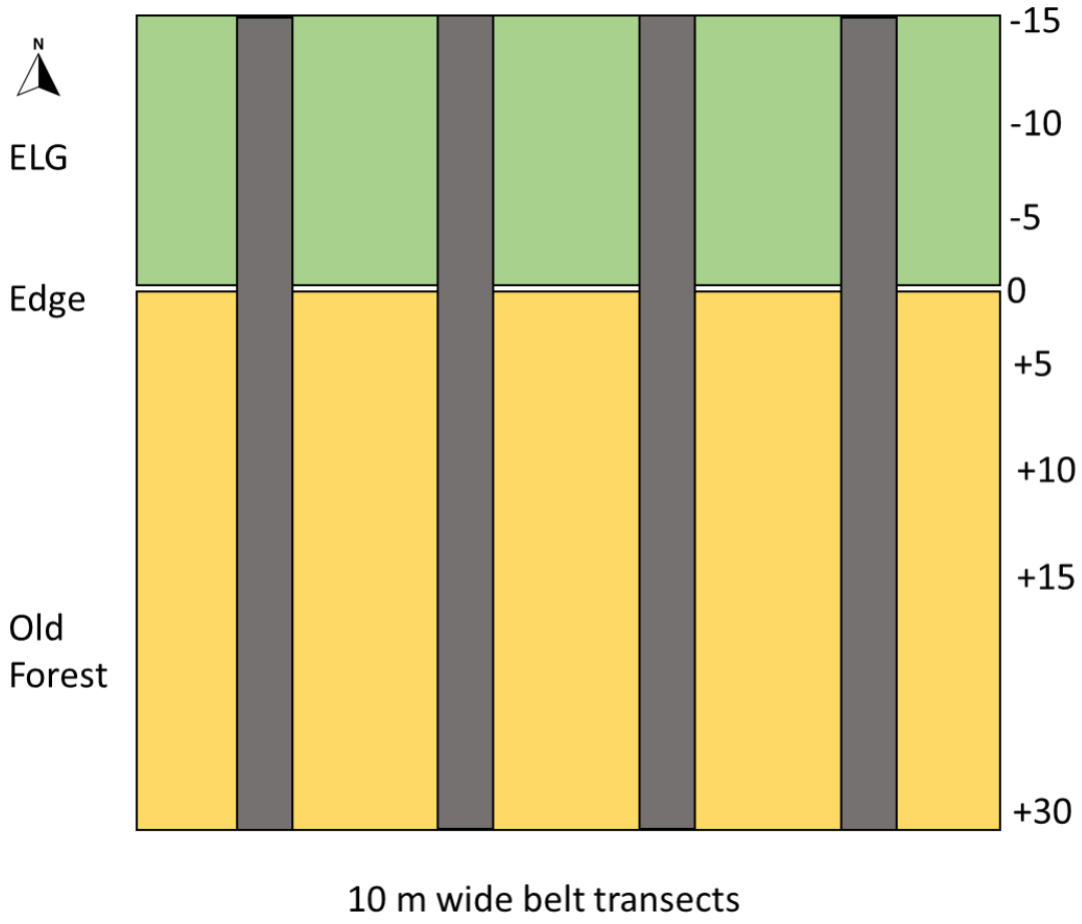

Figure 2. Transect Layout at Yale Myers Forest for Kozy Road and Tree Heaven (aerial view).

The old forest (yellow), the edge, and the ELG (green) are depicted. On the right distances measured in meters are also shown. The mid-line of each transect was located at least 10 m away from any other transect mid-line. Cardinal direction north is indicated.

Leaf Litter Collection and Processing

In the autumn of 2016, leaf litter material was collected at each study location along all four transects at both Kozy Road and Tree Heaven sites (n = 2 sites x 4 transects x 8 locations = 64 samples) by the previously mentioned 0.5 m^2 quadrat frame. The quadrat frame was randomly dropped twice at each study location and all recently senesced litter was collected and placed in labeled paper bags. Leaf litter was homogenized and aerated to dry and prevent mold and halt any decomposition currently taking place during field collections. Leaf litter was dried further in the lab and stored at room temperature, in dry conditions until it was deployed in the autumn of 2017. Litter bags (10 cm x 5 cm) were constructed out of fiberglass coated window screen material with a mesh size of 2 mm^2, which is the standard mesh size for decomposition experimentation and allows microbial/fungal access to the litter. A mass of 6 g of dry leaf litter was placed in each bag. All litterbags were sewn with weather resistant nylon thread and labeled with aluminum tags that were embossed with unique identification numbers.

Litter bags containing site specific litter (i.e., the endemic plant leaf material) were deployed in 2017 one year after initial litter collection. Bags were collected over the next 18 months (2018-2019), collection times: 1, 3, 5, 9, 18 months. A time zero collection was conducted to account for potential transportation effects (e.g., mass loss due to fragmentation during transport), but none were found due to the size of the broad leaf plant litter. After collection litter bags were placed in coolers, then frozen at -20ºC to preserve enzyme integrity and litter composition, to stop any further decomposition, and to preserve the biochemical state at the time of collection. Initially, litter was not dried or heated to preserve extracellular ecoenzymes (EEs), which could be altered by high temperatures. A subsample of the litter material (2 g) was retained and frozen for EE activity assays. The remaining sample mass was processed and prepared for various lab protocols by grinding material to a fine powder using the SPEX® Sample Prep 8000D Mixer/Mill (Spex CertiPrep, Methcuen, NJ USA). Ground samples were weighed for Carbon and Nitrogen elemental analysis and incinerated at 550 ºC in Fisher Scientific Isotemp® Programmable Muffle Furnace (Thermo Fisher Scientific, Waltham, MA USA) to determine the organic matter content via the loss on ignition method.

Soil Collection and Processing

Soil samples were collected at each litterbag collection (i.e., 0, 1, 5, 9, 12, 18 months) throughout the sampling period to provide a surface and subsurface snapshot of the biology at that time in each transect. Five, 5 cm deep soil cores were collected around each litter bag and combined into one sample bag to homogenize the sample and generate a representative sample. This sampling depth allowed soil cores to include the mineral horizon of the soil and not just the litter/humic layer of the soil and was the maximum depth possible because of the rocky subsurface in the sample site environments. Sampling deeper than 5 cm would require significant disturbance to the forest which was not viable. Upon retrieval soil samples were immediately frozen at -20 ˚C in a similar fashion to the corresponding leaf litter samples to enable further testing.

Soil Characterization

To estimate gravimetric soil moisture, 5 g of soil field moist soil was placed in 50 ml glass lab beakers and dried using a BLUE M industrial drying oven (Blue M, New Columbia, PA USA) set to 105°C. Soil weights were taken before drying (grams) and then 24-48 hours after drying to calculate proportion H_2O in the samples.

To estimate soil organic matter content, dry soil samples were heated to 550ºC for 48 hours to combust all organic matter in the sample, leaving only the mineral fraction of the soil. Samples were then weighed again in order to calculate the proportion of organic matter that was lost on ignition. Proportion dry organic matter was calculated by dividing ashed sample weight over dried sample weight. Then, averages of proportion dry organic matter were calculated for distances -15 to 30 for both sites using Excel.

To quantify soil pH, a 1:2 ratio of 25 grams of soil to 50 mL of Mili-Q ultrapure water were placed in 125 mL plastic bottles and mixed on a shaker table for 30 minutes to create a relatively homogenous soil slurry. Soil slurry pH was then taken using a Fisher Scientific Accumet® AB200 pH/mV/Conductivity meter (Thermo Fisher Scientific, Waltham, MA, USA).

Leaf litter elemental analysis

Leaf litter samples were ground using SPEX® Sample Prep 8000D Mixer/Mill (SPEX Certi-Prep, Metuchen, NJ, USA) to a fine powdery consistency, labeled according to their transect number, and stored in capped bottles in dry and cool conditions. The milled litter was then weighed (~2 mg) into tin containers (OD:10 mm; H: 10 mm; Vol.: 785 µL) using a Thermo Scientific Mettler Toledo. XS105 DualRange microscale (Thermo Fisher Scientific, Waltham, MA, USA). Tins were pressed using a pellet press into sealed discs and placed in 96-well standard assay plates in the wells: B1-B10, C1-C10, D1-D10, and E1-E10. Calibration standards with known chemical compositions were placed in wells A1-A10 in order to generate a calibration curve and standardize results. The following were used to prepare the instrument before each run: gas chromatography column conditioner NIST Certified peach leaf material (National Institute of Standards and Technology, NIST-1547, Gaithersburg, MD USA) in order to condition column reagents in preparation for unknowns, two blanks (i.e., empty tins), 0.5 mg acetanilide (National Institute of Standards and Technology, NIST-141E, Gaithersburg, MD USA) 1.0 mg acetanilide, 2.0 mg acetanilide, 1.0 mg cyclohexanone (National Institute of Standards and Technology, CAS No. 108-94-1, Gaithersburg, MD USA), 2.0 mg cyclohexanone, and lastly a mass of cyclohexanone and a mass of NIST Certified pine leaf material (National Institute of Standards and Technology, NIST-1575a, Gaithersburg, MD, USA) that was equivalent to our unknowns in that specific run in the wells A9 and A10 (2 - 5 mg). Similar masses of peach leaves, acetanilide**,** cyclohexanone, and pine were placed in wells, B11-B12, C11-C12, D11-D12, E11-E12 in an alternating fashion as well to serve as check standards to ensure that the instrument was running accurately and that there were no issues with combustion or chromatography. A Thermo Scientific Flash Smart, NC Soil (Thermo Fisher Scientific, Waltham, MA, USA) at Brown University's Environmental Chemistry Laboratory facility was used to measure carbon and nitrogen concentrations of all samples in this study. Five runs containing a total of 180 samples were run over the period of the study.

Conditioner (peach)	Blank	Blank	Acet- 0.5 mg	Acet- 1.0 mg	Acet- 2.0 mg	Cyclo- 1.0 mg	Cyclo- 2.0 mg	Cyclo- = Unk mass	Pine = Unk mass		
unk	unk	unk	unk	unk	unk	unk	unk	unk	unk	C.S.- Peach	C.S.- Acet-
unk	unk	unk	unk	unk	unk	unk	unk	unk	unk	C.S.- Pine	C.S.- Cyclo-
unk	unk	unk	unk	unk	unk	unk	unk	unk	unk	C.S.- Peach	C.S.- Acet-
unk	unk	unk	unk	unk	unk	unk	unk	unk	unk	C.S.- Pine	C.S.- Cyclo-

Figure 3. Leaf Litter Elemental Analysis Assay. Corning black flat bottom 96 well microplate. Visualization of leaf litter elemental analysis performed using the Thermo Scientific Flash Smart, NC Soil at the Brown University Environmental Chemistry Laboratory. Calibration standards are shown in row 1: Conditioner (NIST certified peace leaf material), 2 blanks, 0.5 mg acetanilide, 1.0 mg acetanilide, 2.0 mg acetanilide, 1.0 mg cyclohexanone, 2.0 mg cyclohexanone, a mass equivalent to the mass of the unknown samples being analyzed during that run of cyclohexanone and of NIST certified pine material. Unknown samples undergoing analysis for C and N % are shown in rows 2-5 /columns 1-10. Check standards (C.S.) after each row of unknowns are shown in rows 2-5/columns 11-12. Check standard masses were also equivalent to the mass of the unknown samples being analyzed. Check standards: NIST peach, acetanilide, NIST pine, cyclohexanone. Assay runs sequentially, row by row, beginning with conditioner (NIST peach).

Extracellular Enzyme Activity

Extracellular enzyme activity of hydrolytic ecoenzymes were assayed using methods adapted from the Lab Protocol by Dr. Robert Sinsabaugh (1994) and Dr. Stephen Allison (2005), and later outlined by Bell et al. [24]: Fluorimetric and Oxidative Enzyme Assay Protocol, 10/2012. The presence and activity levels of the enzymes β-glucosidase (BG), Acid Phosphatase (AP), β-N-acetylglucosaminidase (NAG), and β-Xylosidase (XYLO) which are all responsible for carbon and nutrient cycling in soil and leaf litter were tested for. BG catalyzes the rate-limiting step in the hydrolysis reaction of cellobiose to glucose. AP is a hydrolase that catalyzes the hydrolysis of orthophosphate monoesters under acidic conditions into inorganic phosphate, an essential nutrient for plant and animal growth. NAG is responsible for the degradation of chitin; chitin can be found in the exoskeletons of arthropods, shrimps, insects and also in fungi and bacteria. XYLO is an exoglycosidase enzyme that hydrolyzes the non-reducing ends of xylo-oligosaccharides into the more basic form, xylose. Xylose and arabinose are the primary constituents of hemicellulose. Samples were assayed by quantifying rates of catalysis with known substrate polymers. Substrates were fluorescently tagged with 4-Methylumbelliferyl (MUB), and in the presence of their respective enzymes, cleavage by catalysis into their monomeric forms allowed for the quantification of MUB (fluorescent signal), which was read by BioTek Synergy HT (Agilent Technologies, Santa Clara, CA, USA) at 365 nm excitation and 450 nm emission. The substrates solutions: 4-Methylumbelliferyl β-D-glucopyranoside (6.77 mg/100 ml DI water), 4-Methylumbelliferyl phosphate (5.12 mg/100 ml DI water), 4-Methylumbelliferyl N-acetyl-β-D-glucosaminide (7.59 mg/100 ml DI water), and 4-Methylumbelliferyl β-D-xylopyranoside (6.17 mg/100 ml DI water), respectively. The MUB standard solution was made by dissolving 1.17 mg of 4-Methylumbelliferyl in 1 ml acetone, and then adding 100 ml DI water. Substrates solutions were refrigerated and used within 5 days of preparation, which is in agreement with published protocols. A pH buffer was prepared to control variation in sample pH. The buffer was comprised of 50 mM sodium acetate (13.608 g sodium acetate trihydrate) and pH was adjusted using 1M glacial acetic acid (pH=5).

Assay samples were prepared by adding 2 g of field moist soil to 100 ml sodium acetate buffer in a 250 ml bottle. The solution was then mixed thoroughly for 20 minutes on a mechanical shaker table. The solution was then emptied into a glass dish and spun via magnetic

stir rod using a Thermolyne Nuova II Stir Plate until the solution became a homogenous slurry. Slurries were pipetted into assay plates within 30 minutes. Enzyme assays were conducted using Corning black flat bottom 96 well microplates (Corning® 96-well Solid Black Flat Bottom Polystyrene TC-treated Microplates, Corning, NY US) were labeled with lab tape according to which enzyme would be tested for in that plate (i.e., BG, AP, NAG, and Xylo). Multiple samples are run in a single plate, multiple plates for each enzyme were often used and labeled in order to maximize efficiency (i.e., BG 1, BG 2, BG 3, etc.) Using multichannel pipettors and wide-mouth tips (cut by hand), 200 µl of soil slurry from each sample being run was pipetted into the 96 well plates while keeping the slurry homogenized throughout the duration of pipetting. As previously stated, each 96 well plate can test 3 samples at a time. 200 µl of sample 1 was pipetted into all wells in columns 4-6, 200 µl of sample 2 in columns 7-9, and 200 µl of sample 3 in columns 10-12. Next, 250 µl of sodium acetate buffer was added to all wells in column 1, 200 µl of buffer was added into columns 2 and 3, and lastly 50 µl of buffer was added into columns 4, 7, and 10. Next, 50 µl of MUB was added to all wells in columns 2, 5, 8, and 11. At this point assay plates could be stored in the refrigerator, for 5 days or less, until substrate solutions were prepared and ready to be pipetted. Prior to incubation, 50 µl of respective substrate solution was pipetted into all wells in columns 3, 6, 9, and 12 where the assays were taken place. All wells now held 250 µl.

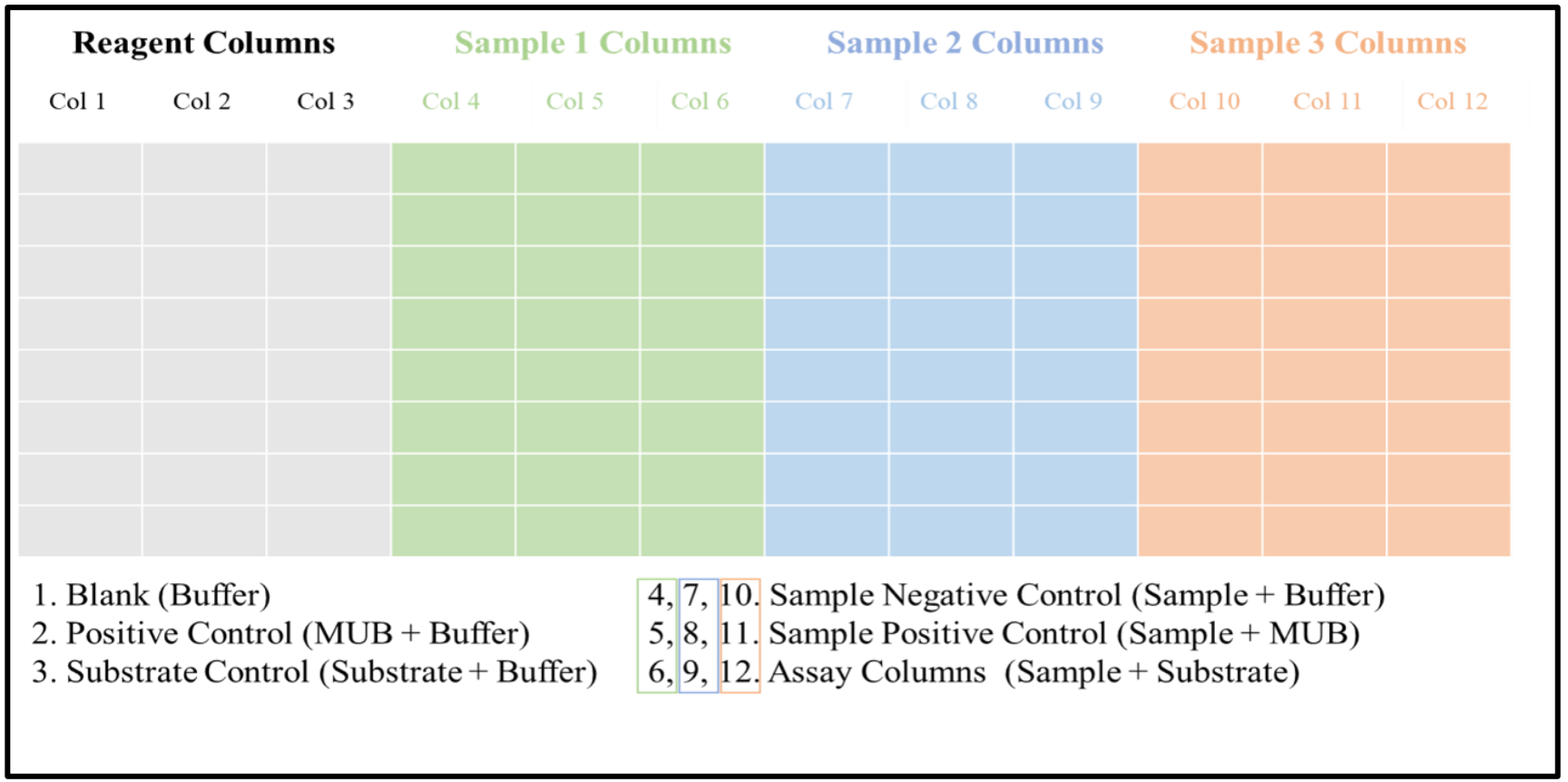

Figure 4. Extracellular Enzyme Activity Assay.

Corning black flat bottom 96 well microplate. Visualization of the Fluorimetric and Oxidative Enzyme Assay Protocol. Grey shading represents controls free of sample material, while green, blue and peach shading represent three distinct samples and associated buffer, standard, and substrate wells. Column averages were used to estimate the activity of β-glucosidase, Acid Phosphatase, β-N-acetylglucosaminidase, and β-Xylosidase (Figure from D. Hewins).

Plates were incubated at room temperature for 4 hours to allow for maximum enzyme catalysis (incubation time varies depending on sample type). Plates were read for fluorescence using a BioTek Synergy HT at 365 nm excitation and 450 nm emission. Extracellular enzyme activity (EEA) data was then recorded in an excel sheet for later analysis**.** In order to ensure fluorescence was due to MUB activity net fluorescence was calculated using the following equation:

NFU= {(Assay-Sample)/ [Quench Control-Sample)/ Standard]} - Substrate

(Eqn. 1)

NFU was then inputted into the equation for calculating extracellular enzyme activity:

Activity (µmol $h^{-1}g^{-1}$) = {NFU/ [Standard FU/ 10 µmol/L x 0.0005)]} / [0.0002 L x (DW g/ 0.100 L) x 4]

(Eqn. 2)

Activity in assay wells 6, 9, and 12 were calculated for 2 g soil samples and for proportion dry organic matter averages. Dry organic matter averages were calculated for distances -15 to 30 for both Kozy Road and Tree Heaven. Extracellular enzyme activity assays were calculated on a per gram soil (2g field moist) and a per gram soil organic matter basis for all soil samples assayed in this study to evaluate activity

Results

For the purpose of this thesis we are presenting descriptive statistics (averages, standard errors) and plan to conduct more intensive hypothesis testing and multivariate statistics as we prepare a manuscript in the coming months.

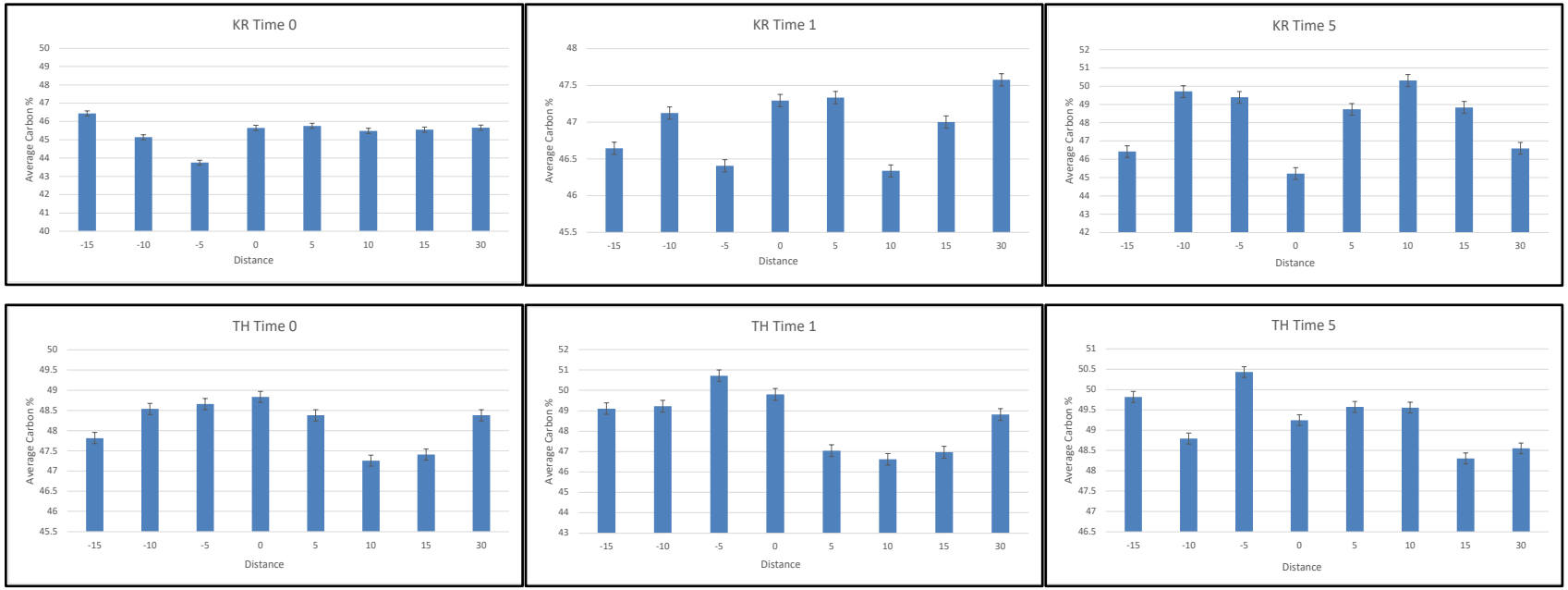

Figure 5. Average Carbon Percentage of Leaf Litter for Kozy Road and Tree Heaven

Average carbon percentage for Kozy Road and Tree Heaven for collection times zero through five. Overall average C percentage for each distance is shown. Distances are measured in meters. Maximum C percentage was found in TH: >50% at time 1, distance -5). KR's overall average C percentage across all distances and collection times rose from 45.420 to 48.152 %. TH's overall average C percentage rose from 48.158 to 49.241 %. KR standard deviation: (T0- 0.7699)(T1- 0.4560)(T5- 1.8285). TH SD: (T0- 0.5907)(T1- 1.4936)(T5- 0.7072).

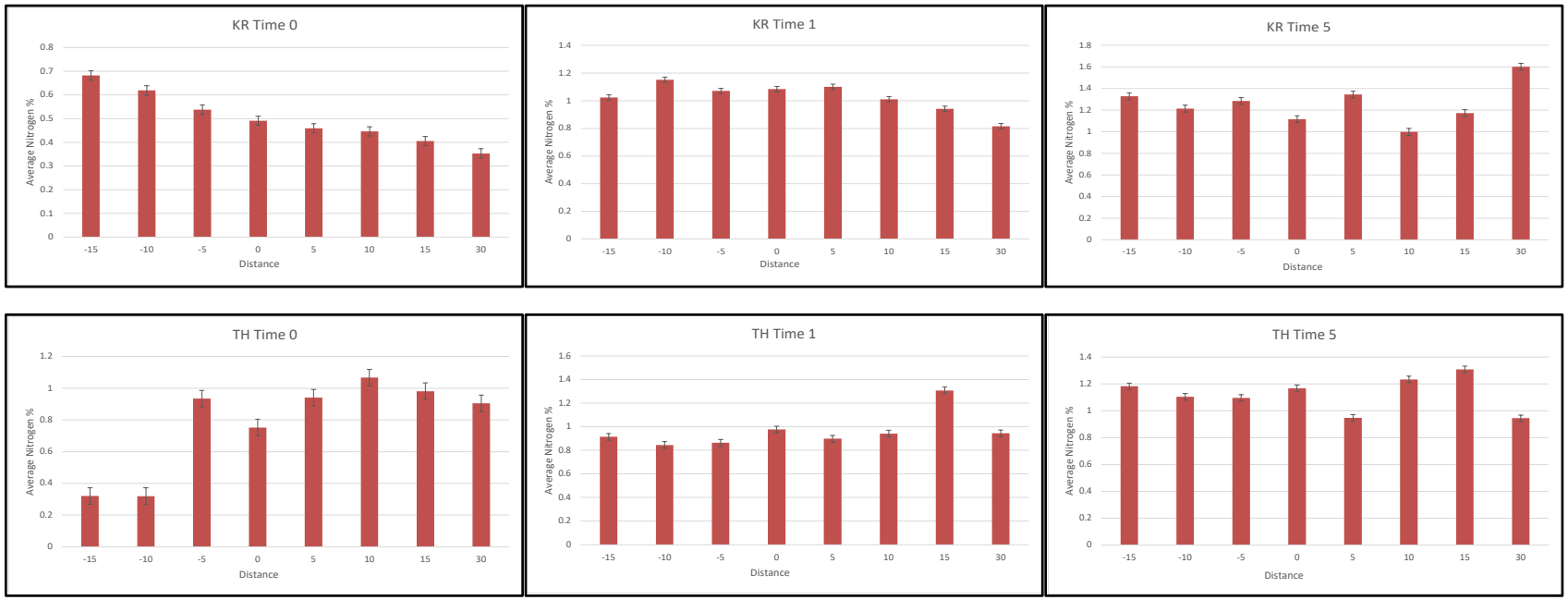

Figure 6. Average Nitrogen Percentage of Leaf Litter for Kozy Road and Tree Heaven

Average Nitrogen percentage for Kozy Road and Tree Heaven for collection times zero through five. Overall average N percentage for each distance is shown. Distances are measured in meters. Overall average N percentages rose in both sites over the course of the three collection periods. KR's overall N percentage was slightly higher by collection time 5 (KR: 1.258 and TH: 1.088). KR's overall average N percentage rose from 0.05041 to 1.258 %. TH's overall average N percentage rose from 0.777 to 1.088 %. Overall N percentages for both sites reach values of ~ 1% by the end of the study (maximum KR Time 5: ~1.6%). KR SD: (T0- 0.1093)(T1- 0.1058)(T5- 0.1800). TH SD: (T0- 0.2958)(T1- 0.1462)(T5- 0.1285).

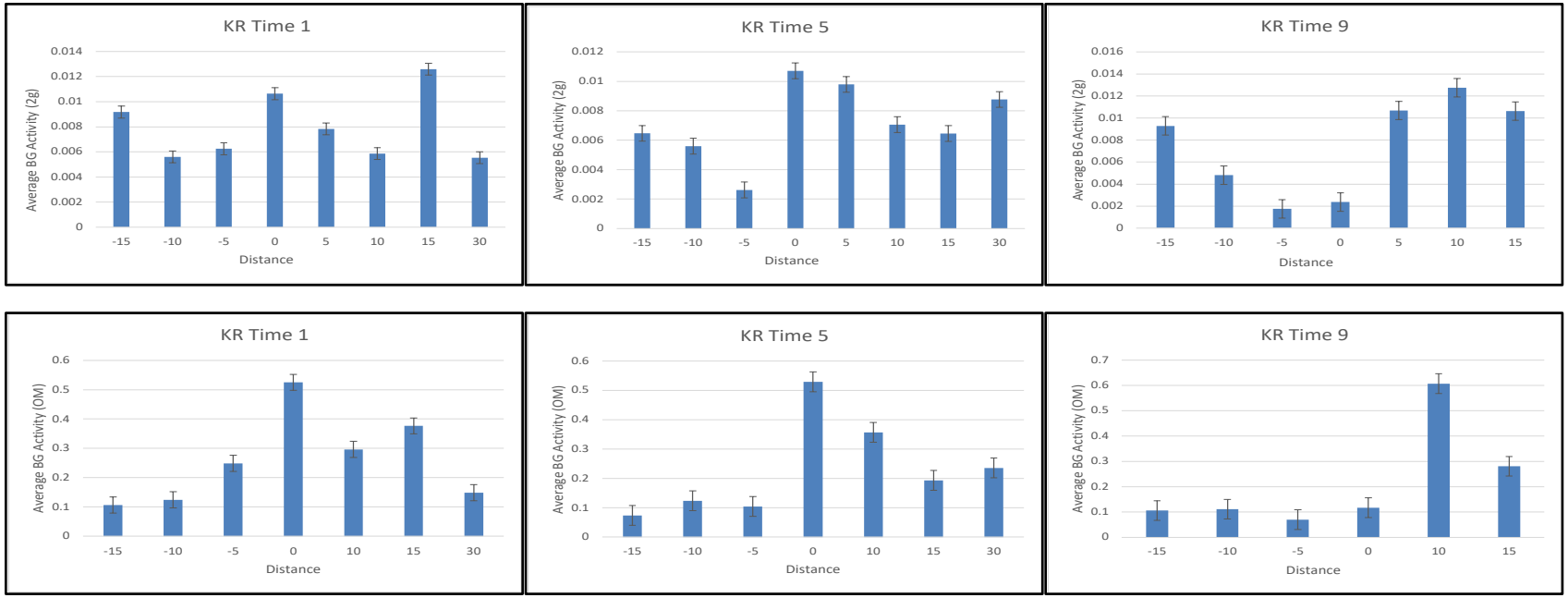

Figure 7. Average Extracellular Enzyme Activity for *β*-glucosidase in Kozy Road.

Average EEA for BG in Kozy Road for collection times one through nine. Overall average BG EEA for each distance is shown. Distances are measured in meters. Extracellular enzyme activity is measured in μmol $h^{-1}g^{-1}$. *β*-glucosidase EEA values for 2g and proportion organic matter soil samples from KR showed a decrease in the ELG when compared to the old-growth forest across all collection times. Overall average EEA levels for BG in OM declined from a value of 0.2608 to 0.2153 μmol $h^{-1}g^{-1}$. Whereas 2g soil samples decreased initially, but then increased: (0.0079 – 0.0068 – 0.0075 μmol $h^{-1}g^{-}$). KR 2g SD: (T1- 0.0026)(T5- 0.0025)(T9- 0.0044). KR OM SD: (T1- 0.1527)(T5- 0.1624)(T9- 0.2056).

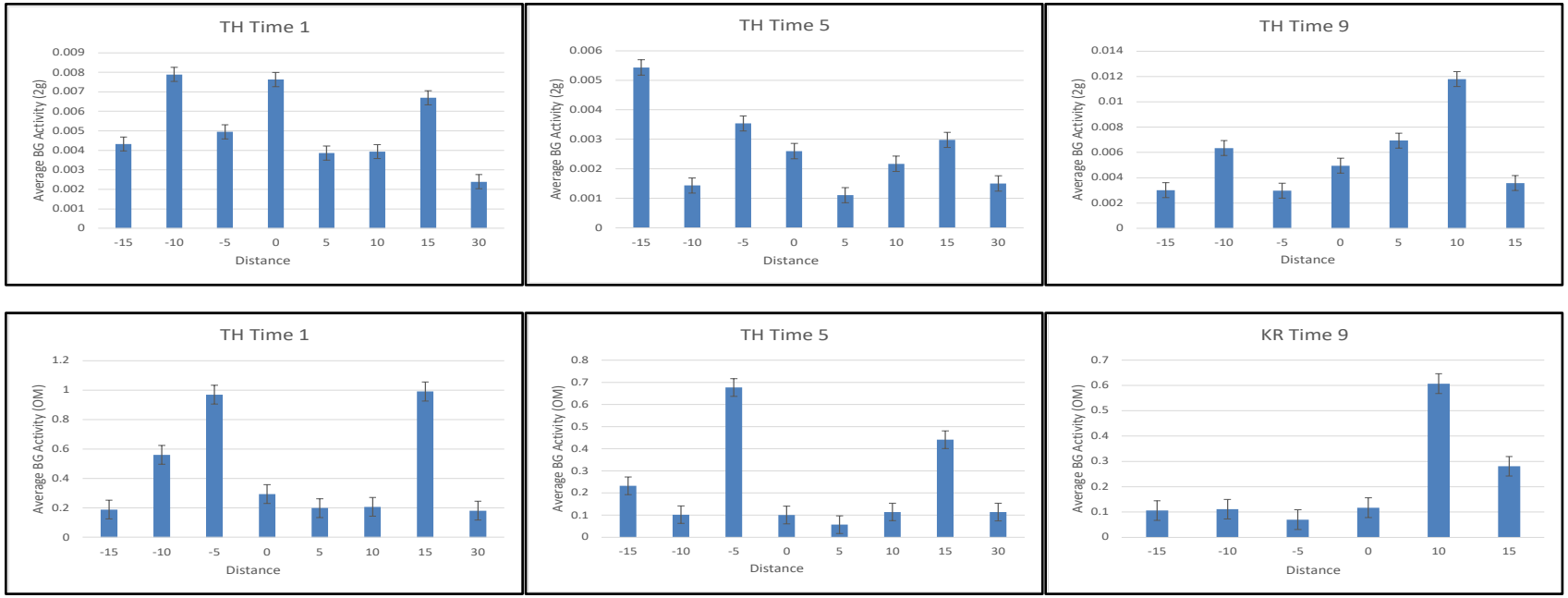

Figure 8. Average Extracellular Enzyme Activity for *β*-glucosidase in Tree Heaven.

Average EEA for BG in Tree Heaven for collection times one through nine. Overall average BG EEA for each distance is shown. Distances are measured in meters. Extracellular enzyme activity is measured in µmol $h^{-1}g^{-1}$. *β*-glucosidase EEA values for 2g and proportion organic matter soil samples from TH showed a trend of increasing EEA from distance (-15) to distance (0) for times 1 and 5. Values decreased dramatically after distance (0) for times 1 and 5. Overall average EEA levels for BG in OM declined initially, but then increased: (0.4653 – 0.2393 – 0.3680 µmol $h^{-1}g^{-1}$). Overall average EEA levels for BG in 2g soil samples also declined initially, but then increased: (0.0079 – 0.0068 – 0.0075 µmol $h^{-1}g^{-1}$). TH 2g SD: (T1- 0.0019)(T5- 0.0014)(T9- 0.0031). TH OM SD: (T1- 0.3506)(T5- 0.2186)(T9- 0.1914).

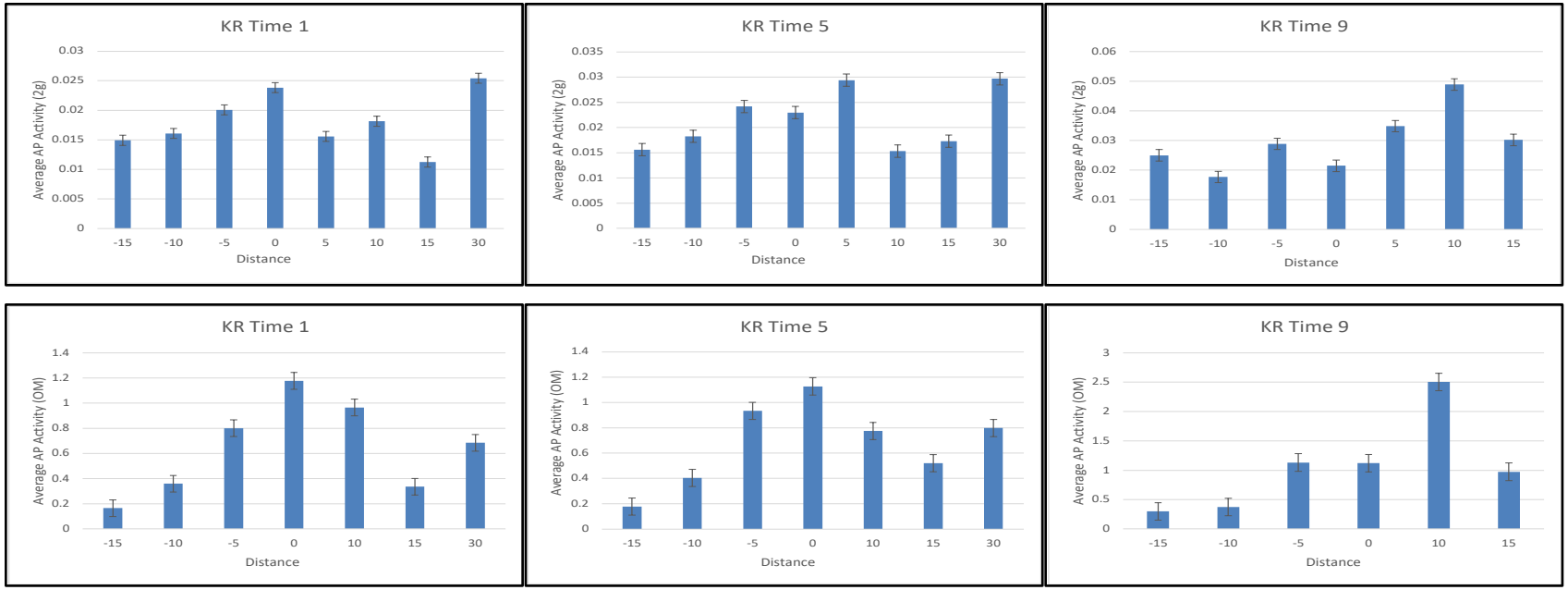

Figure 9. Average Extracellular Enzyme Activity for Acid Phosphatase in Kozy Road.

Average EEA for AP in Kozy Road for collection times one through nine. Overall average AP EEA for each distance is shown. Distances are measured in meters. Extracellular enzyme activity is measured in µmol $h^{-1}g^{-1}$. Acid Phosphatase EEA values for 2g and proportion organic matter were significantly higher than BG EEA values. Extracellular enzyme activity values for AP in KR showed a trend of increasing values from distance (-15) to distance (0), before decreasing gradually, for collection times 1 and 5 (maximum EEA at distance 0). Overall average EEA for AP in KR shows a shift in the maxima for EEA from the forest edge to deeper into the old-growth forest by time 9. Overall average EEA levels for AP in OM showed an increasing linear trend across the study period ranging from an initial value of 0.6411 to 1.0669 µmol $h^{-1}g^{-1}$. Overall average EEA levels for AP in 2g also showed an increasing linear trend ranging from 0.0182 to 0.0295 µmol $h^{-1}g^{-1}$. KR 2g SD: (T1- 0.0047)(T5- 0.0058)(T9- 0.0102). KR OM SD: (T1- 0.3690)(T5- 0.3267)(T9- 0.7937)

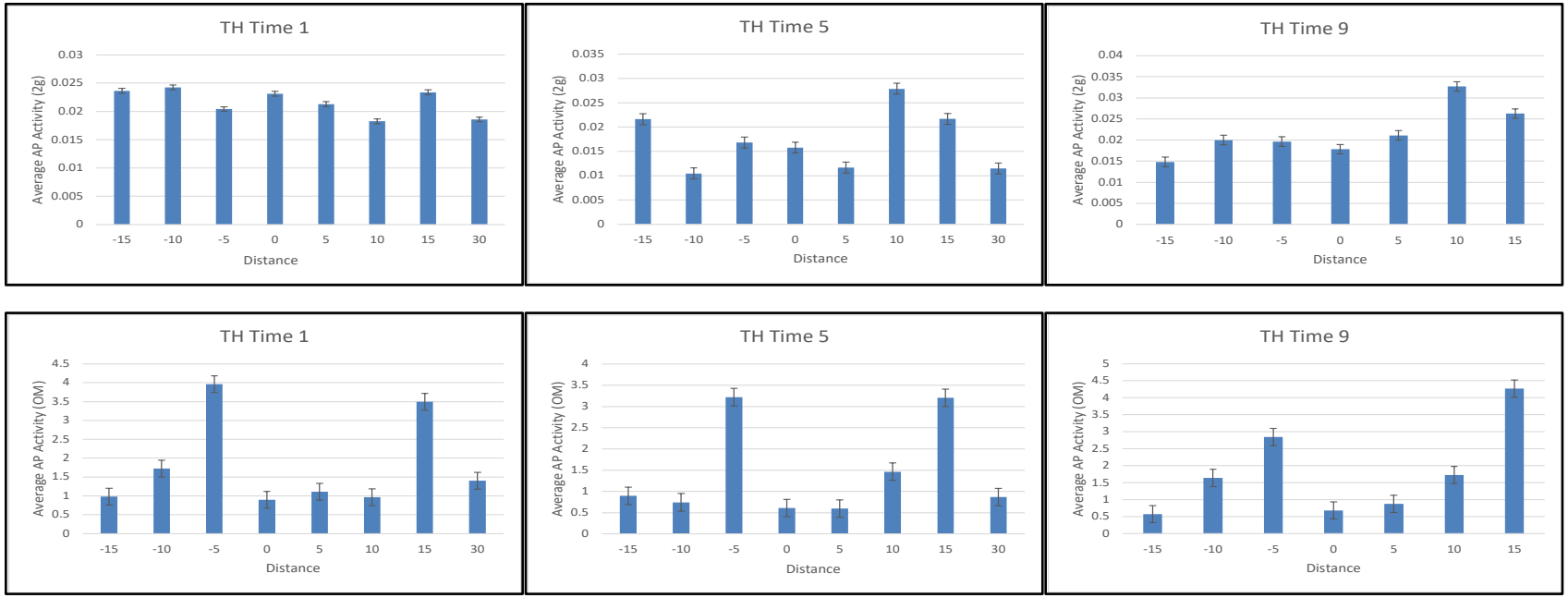

Figure 10. Average Extracellular Enzyme Activity for Acid Phosphatase in Tree Heaven.

Average EEA for AP in Tree Heaven for collection times one through nine. Overall average AP EEA for each distance is shown. Distances are measured in meters. Extracellular enzyme activity is measured in μmol $h^{-1}g^{-1}$. The highest measured EEA value for all ecoenzymes of 4.25 μmol $h^{-1}g^{-1}$ was found in an OM soil sample from the old-growth forest in TH, during the time 9 collection period. Extracellular enzyme activity values were also slightly higher in TH when compared to KR for AP. Extracellular enzyme activity values for AP in proportion organic matter increased up until distance (0), upon which values dropped back down to initial levels before beginning to rise again. Overall average EEA levels for OM values: (1.8721 – 1.4786 – 1.8012 μmol $h^{-1}g^{-1}$). Overall average EEA levels for 2g values: (0.0217 – 0.0170 – 0.0218 μmol $h^{-1}g^{-1}$). TH 2g SD: (T1- 0.0023)(T5- 0.0061)(T9- 0.0059). TH OM SD: (T1- 1.2157)(T5- 1.1214)(T9- 1.3425).

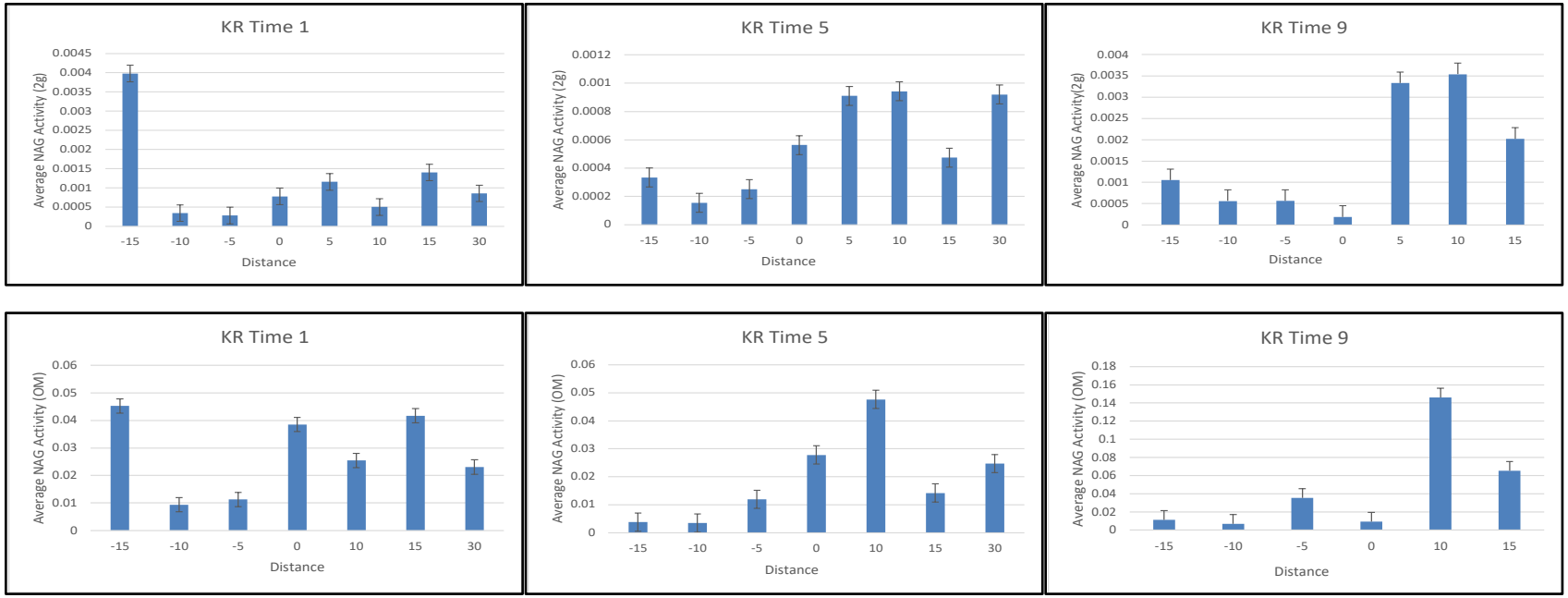

Figure 11. Average Extracellular Enzyme Activity for *β*-N-acetylglucosaminidase in Kozy Road.

Average EEA for NAG in Kozy Road for collection times one through nine. Overall average NAG EEA for each distance is shown. Distances are measured in meters. Extracellular enzyme activity is measured in μmol $h^{-1}g^{-1}$. *β*-N-acetylglucosaminidase EEA values for 2g and proportion organic matter were significantly lower than EEA values for BG and AP. Extracellular enzyme activity values were markedly higher in the old-growth forest when compared to the ELG across all collection times in KR for NAG. Overall average EEA values for NAG in OM showed a decreasing trend, followed by an increase: (0.0278 – 0.0191 – 0.0457 μmol $h^{-1}g^{-1}$). Overall average EEA values for NAG in 2g showed a similar trend: (0.0012 – 0.0005 – 0.0016 μmol $h^{-1}g^{-1}$). KR 2g SD: (T1- 0.0012)(T5- 0.0003)(T9- 0.0013). KR OM SD: (T1- 0.0144)(T5- 0.0156)(T9- 0.0539).

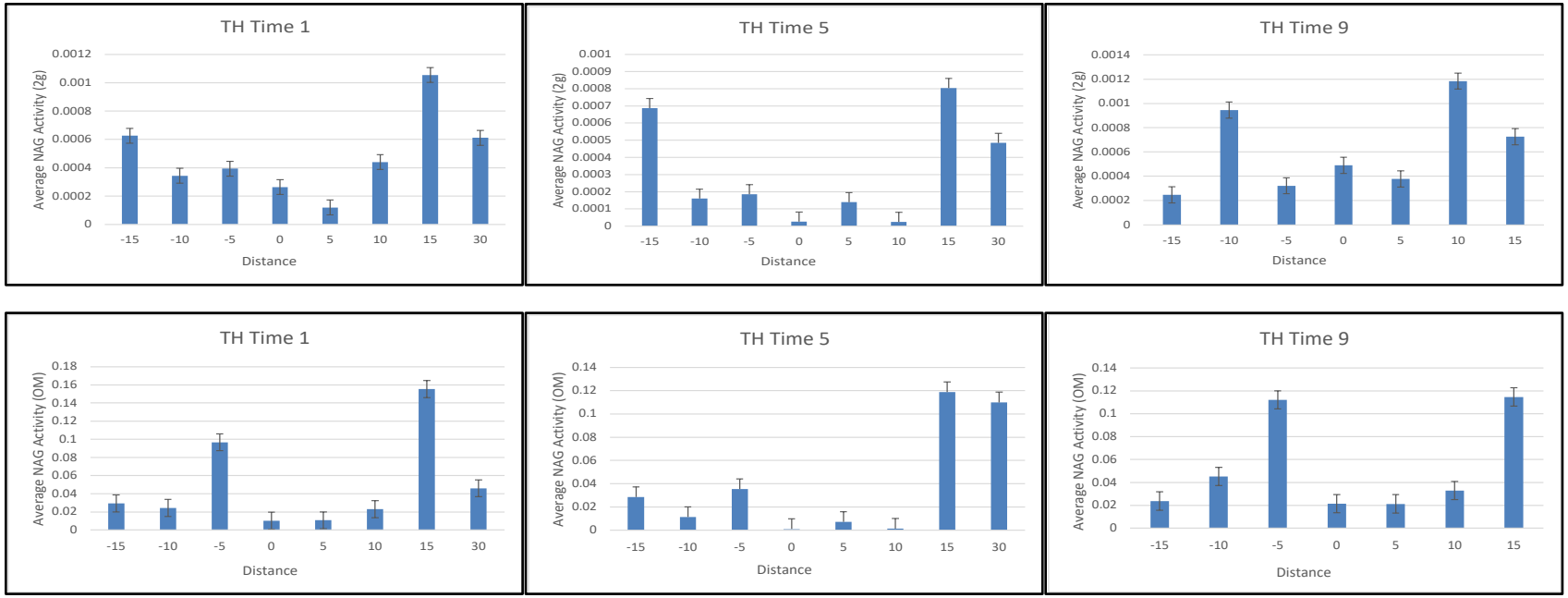

Figure 12. Average Extracellular Enzyme Activity for *β*-N-acetylglucosaminidase in Tree Heaven.

Average EEA for NAG in Tree Heaven for collection times one through nine. Overall average NAG EEA for each distance is shown. Distances are measured in meters. Extracellular enzyme activity is measured in µmol $h^{-1}g^{-1}$. *β* -N-acetylglucosaminidase EEA values for 2g and proportion organic matter in TH showed the highest values at the edges of the study site (distances -15, +15, and +30) for collection times 1 and 5, with +15 remaining the maxima throughout. However, no significant difference was found between the ELG and the old-growth forest for the 2g data set in time 9 in TH. Overall average EEA values for Nag in OM: (0.0510 – 0.0415 – 0.0531 µmol $h^{-1}g^{-1}$). Overall average EEA values for Nag in 2g showed a similar trend: (0.0005 – 0.0003 – 0.0006 µmol $h^{-1}g^{-1}$). TH 2g SD: (T1- 0.0002)(T5- 0.0003)(T9- 0.0004). TH OM SD: (T1- 0.0510)(T5- 0.0480)(T9- 0.0420).

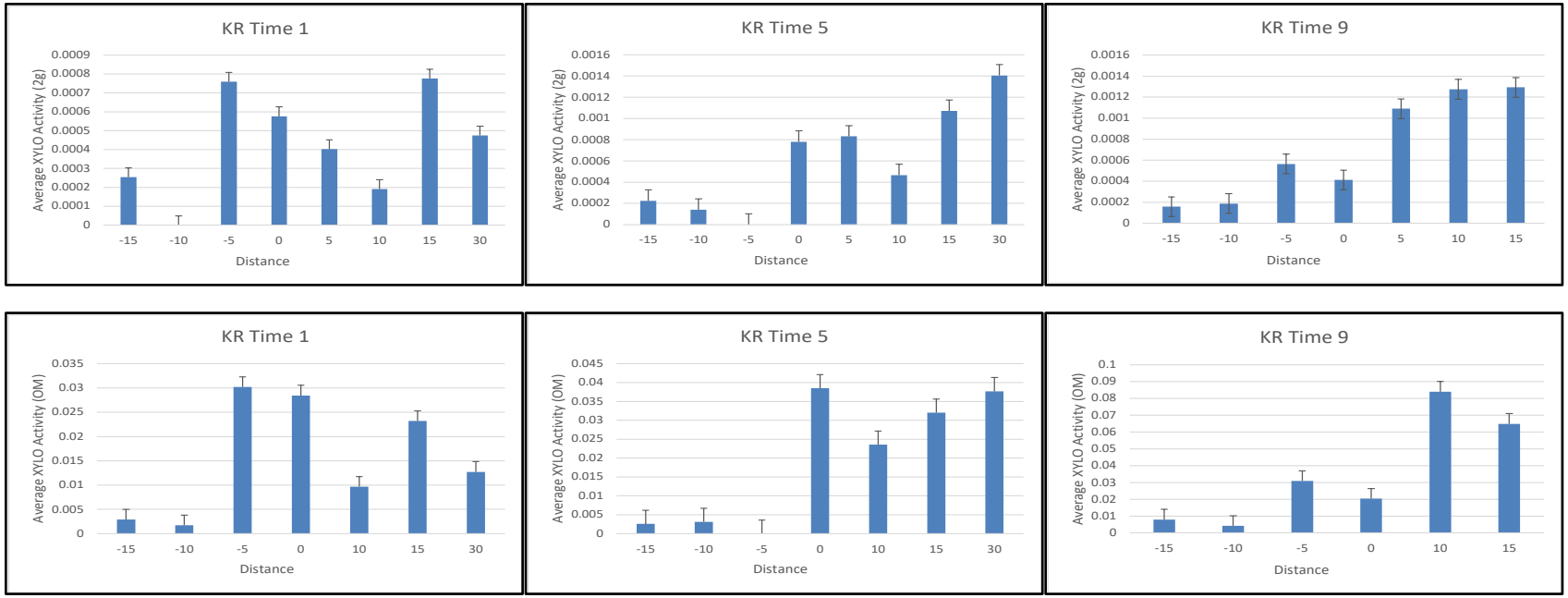

Figure 13. Average Extracellular Enzyme Activity for *β*-Xylosidase in Kozy Road.

Average EEA for XYLO in KR for collection times one through nine. Overall average XYLO EEA for each distance is shown. Distances are measured in meters. Extracellular enzyme activity is measured in µmol $h^{-1}g^{-1}$. *β*-Xylosidase EEA values for 2g and proportion organic matter in KR values were the lowest of all 4 EEs. Extracellular enzyme activity levels showed higher values in the old-growth forest when compared to the ELG in KR, especially collection times 5 and 9. Overall average EEA values for XYLO in OM increased linearly from 0.0155 to 0.0353 µmol $h^{-1}g^{-1}$. Overall average EEA values for XYLO in 2g increased linearly from 0.0004 to 0.0007 µmol $h^{-1}g^{-1}$. KR 2g SD: (T1- 0.0002)(T5- 0.0004)(T9- 0.0005). KR OM SD: (T1- 0.0117)(T5- 0.0173)(T9- 0.0322).

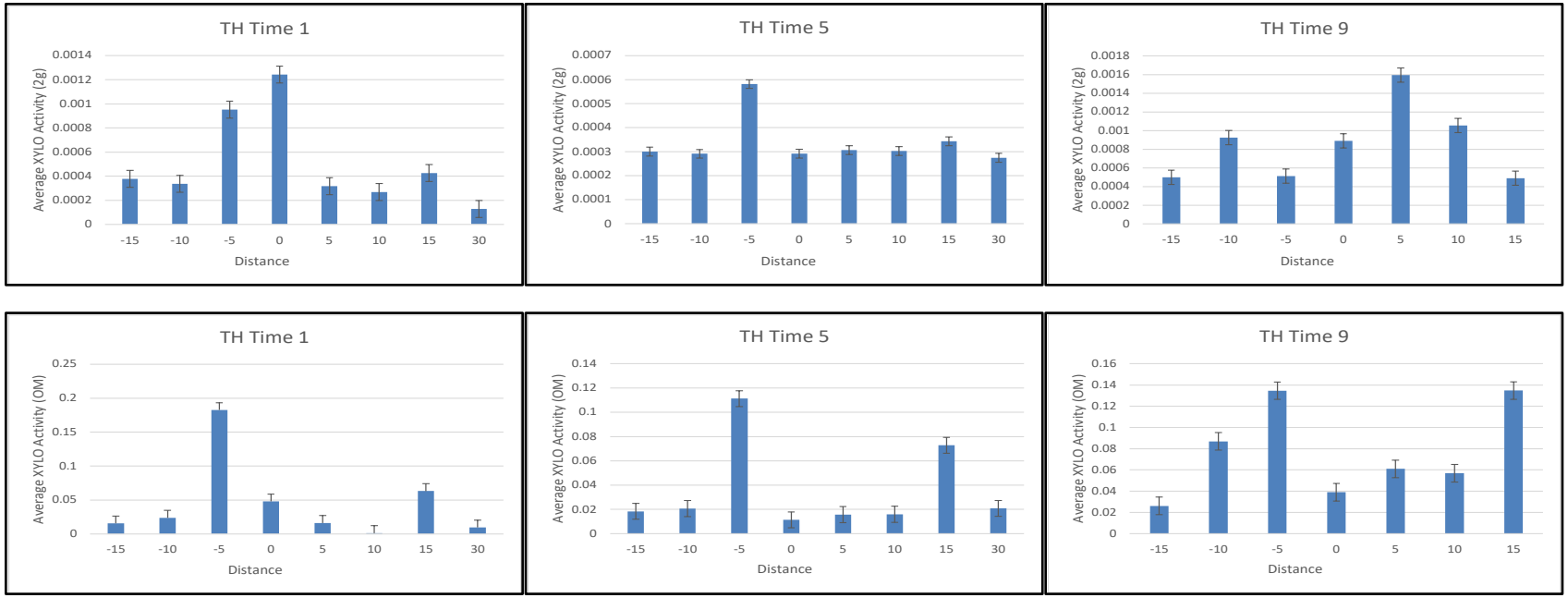

Figure 14. Average Extracellular Enzyme Activity for *β*-Xylosidase in Tree Heaven.

Average EEA for XYLO in TH for collection times one through nine. Overall average XYLO EEA for each distance is shown. Distances are measured in meters. Extracellular enzyme activity is measured in µmol $h^{-1}g^{-1}$. Extracellular enzyme activity values for XYLO taken in TH show no significant difference in EEA values between the ELG and the old-growth forest for both 2g and OM data sets. Extracellular enzyme activity values increased from distance (-15) to distance (0), decreased, and then rose again deeper into the old-growth forest for XYLO at TH during time 9. Overall average EEA values for XYLO in OM decreased initially, and then increased: (0.0475 – 0.0372 – 0.0778 µmol $h^{-1}g^{-1}$). Overall average EEA values for XYLO in 2g followed a similar trend: (0.0005 – 0.0003 – 0.0009 µmol $h^{-1}g^{-1}$). TH 2g SD: (T1- 0.0003)(T5- 0.0001)(T9- 0.0004). TH OM SD: (T1- 0.0591)(T5- 0.0362)(T9- 0.0436).

Conclusions

With the aim of better understanding the potential long-term implications of forest logging on ecosystem function and soil biogeochemistry, and to elucidate whether differences in edaphic conditions and soil biotic activity due to disturbance could be observed between the ELG and the adjacent 100 + year old forest we conducted a range of measurements in the field and laboratory. Leaf litter samples collected from the study sites Kozy Road (KR) and Tree Heaven (TH) underwent elemental analysis to measure the change in litter carbon and nitrogen throughout the experiment, which highlights mineralization and immobilization of C and N over time. Soil samples were collected at each litterbag collection throughout the sampling period to provide a surface and subsurface snapshot of the biology at that time in each transect.

Carbon and Nitrogen Elemental Analysis

Litter samples were collected from (-15) m into the experimental large gap (ELG) to (+30) m into the old-growth forest. Samples represented three collection times: zero months (a time zero collection was conducted to account for potential transportation effects, but none were found due to the size of the broad leaf plant litter), one month and five months after original collection. A total of five runs containing 180 samples were analyzed.

When comparing C percentages in KR between the ELG and the old-growth forest no significant differences were found. When comparing C percentages in TH between the ELG and the old-growth forest higher values were found to be associated with the ELG than with the old-growth forest. Values rose from the edge of the ELG (distance -15) up until about the forest edge, in which case values then dropped.

Overall C percentages rose across all sites and throughout all collection times, with TH having marginally higher values by time five. Tree Heaven's marginally higher overall value for C may possibly be due to its differing plant community when compared to KR [23]. The trend of rising C percentage may be due to the inherent sequential process of decomposition. Early on in the decomposition process, easily digestible labile organic compounds are decomposed first. Thus, leaving the remaining organic material to be transformed into a more recalcitrant humic layer in the soil.

The rising trend of C percentage may indicate a higher overall relative abundance of C. A higher concentration of recalcitrant C leads to the possible accumulation of C in the leaf litter and may contribute to the accumulation of soil organic matter (SOM) in the form of the humic soil layer. Organic matter affects the physical, chemical, and biological properties of soil and is of vital importance to the overall health of forest ecosystems. SOM improves soil quality by increasing water and nutrient retention which results in greater net primary production (NPP) in plants. It also improves soil structure which in turn may reduce erosion, nutrient leaching, and lead to an improvement in ground and surface water quality. Soil organic matter is especially important in New England forests where the majority of humic soils are thin and underlaid with bedrock. Proper management, conservation, and restoration practices of soil organic carbon and SOM levels in forest ecosystems directly impact the exponential increase of CO_2 in the atmosphere [4].

Overall average N percentages rose in both sites over the course of the three collection periods as well. Nitrogen values for KR time 0 show a clear decreasing linear trend with the highest value associated with the ELG (distance -15: ~ 0.68%) and the lowest value associated with the old-growth forest (distance +30: 0.36%). This trend may also indicate the

immobilization of Ns in the soil. Nitrogen immobilization and mineralization is the process in which soil microbes convert organic N found in decaying plant matter into inorganic forms that may be readily taken up by living plants [25]. Nitrogen in forest soils limits the rate of NPP, is an essential nutrient for plant and animal growth, and is an essential component of enzymes that are responsible for mediating the biogeochemical reactions that lead to a reduction in C (e.g., photosynthesis) [6]. Thus, elevated N in litter and soil suggest that N, which is a limited resource, is likely occluded in recalcitrant organic matter.

Extracellular Enzyme Activity

Soil samples collected from TH and KR were analyzed for the presence of 4 ecoenzymes (EE) that play a major role in carbon and nutrient cycling in soil as explained previously: β-glucosidase (BG), Acid Phosphatase (AP), β-N-acetylglucosaminidase (NAG), and β-Xylosidase (XYLO). Soil samples were collected over 3 time intervals: 1 month (1 month after the initial deployment of litter in this study), 5 months, and 9 months. Soil samples weighing 2 g (field moist soil) were analyzed for extracellular enzyme activity (EEA). Extracellular enzyme activity occurring in just the organic proportion of the soil samples was then measured as well. EE hydrolyze bonds in organic matter (OM) specifically, and thus a more accurate measurement of their EEA can be assessed by measuring EEA in just the organic portion of the soil samples. Extracellular enzyme activity was measured in μmol $h^{-1}g^{-1}$ and average values were calculated for all distances in all sites.

Firstly, EEA values were the highest in the OM proportion for all soil samples, across all collection times, and throughout both sites as expected. Trends in the EEA data were usually consistent between 2g and OM sample sets. However, OM data allowed for better visualization of these trends with less noise and/or potential confounding factors.

The highest EEA values were found for the EEs BG and AP across both study sites and throughout all collection times. This result may be explained by the fact that BG hydrolyzes cellulose, which is the most abundant material found in litter and soils in forests. Acid Phosphatase works upon organic phosphorus and converts it into its inorganic form, an essential nutrient for all life as discussed previously. If enough readily and easily digestible substances can be found decomposer organisms such as fungi will not bother to excrete EEs such as XYLO and NAG.

Ecoenzymes NAG and XYLO were found in very limited amounts relatively and may reflect the above conclusion. β-Xylosidase acts to hydrolyze more recalcitrant compounds like lignin and other immobilized materials. β-N-acetylglucosaminidase acts to hydrolyze chitin, a tough material found in the exoskeletons of arthropods, shrimps, insects and also in fungi and bacteria. Given that these materials are more structurally complex and difficult to breakdown, its likely that organisms are accessing energy (carbon) and nutrients from other more available sources.

Limitations to this study may be the relatively short length of time (0-9 months) and relatively small sample size (180 samples for elemental analysis and 172 soil samples for EEA). Stark patterns in C:N and EEA may be best seen in longer studies considering the nature of the decomposition process and climate conditions in New England. Further testing of KR and TH may indicate stronger associations between clearcutting and its effect on the biogeochemical cycles in New England Forests. In the coming months, we plan to continue to measure and collect data from samples collected beyond the nine month cutoff for this study extending data collection to 12 and 18 months.

Acknowledgements

First and foremost, I would like to thank Dr. Hewins for his continued support and mentorship. Without his acceptance, guidance, and consistent belief in my research abilities I would have never achieved all that I have at Rhode Island College. Dr. Hewins allowed me to realize my full potential and I will be forever grateful. I would also like to thank Dr. Roberts for being such a friendly, down to earth, and immensely helpful person. Dr. Roberts was my first advisor when I transferred to Rhode Island College, and he immediately went to bat for me. Dr. Roberts, thank you so much for welcoming me into the biology program and for being the great man that you are. I would also like to thank and honor all of the professors I had and met during my time at Rhode Island College. The personal engagement and high expectations all of my professors provided were essential in my growth as a scientist, thank you. I would also like to thank Jessica Clark, my lab mate in Dr. Hewins lab, for the countless hours of comradery and the lab work she performed. Lastly, I would like to thank my family, friends, and loved ones. I am so lucky to have so many loving and supportive people in my life. This is only the beginning, thank you!

References

1. Herring, D. (2012, March 6). *Climate change: Global temperature projections*. NOAA Climate.gov. Retrieved April 2, 2023, from https://www.climate.gov/news-features/understanding-climate/climate-change-global-temperature-projections

2. Environmental Protection Agency. (2022, May 16). *Overview of Greenhouse Gases*. EPA. Retrieved April 2, 2023, from https://www.epa.gov/ghgemissions/overview-greenhouse-gases

3. Dahlman, R. L. A. N. D. L. A. (2023, January 18). *Climate change: Global temperature*. NOAA Climate.gov. Retrieved April 2, 2023, from https://www.climate.gov/news-features/understanding-climate/climate-change-global-temperature

4. Ontl, T. A. (2012). *Soil Carbon Storage*. Nature news. Retrieved April 2, 2023, from https://www.nature.com/scitable/knowledge/library/soil-carbon-storage-84223790/

5. Dobrijevic, D. (2022, March 29). *The lithosphere: Facts about Earth's outer shell*. Space.com. Retrieved April 2, 2023, from https://www.space.com/lithosphere-earth-outer-layer

6. Schlesinger, W. H. (1997). *Biogeochemistry an analysis of global change*. Academic Press.

7. CLIMATETRADE Corp. Sucursal en España. (2023, January 25). *Which countries are the world's biggest carbon polluters?* ClimateTrade. Retrieved April 2, 2023, from https://climatetrade.com/which-countries-are-the-worlds-biggest-carbon-polluters/

8. Monger, H. C., Daugherty, L. R. A., Lindemann, W. C., & Liddell, C. M. (1991). Microbial precipitation of pedogenic calcite. *Geology*, *19*(10), 997. https://doi.org/10.1130/0091-7613(1991)019<0997:mpopc>2.3.co;2

9. Monger, H., & Martinez-Rios, J. (2000). Inorganic carbon sequestration in Grazing Lands. *The Potential of U.S. Grazing Lands to Sequester Carbon and Mitigate the Greenhouse Effect*. https://doi.org/10.1201/9781420032468.ch4

10. Schlesinger, W. H. (1997). *Biogeochemistry an analysis of global change*. Academic Press.

11. SONG Piao 宋飘, ZHANG Naili 张乃莉, MA Keping 马克平, & GUO Jixun 郭继勋. (2014). Impacts of global warming on litter decomposition. *Acta Ecologica Sinica*, *34*(6). https://doi.org/10.5846/stxb201210251479

12. Allison, S. D., Gartner, T. B., Holland, K., Weintraub, M., & Sinsabaugh, R. L. (2007). Soil enzymes: Linking proteomics and Ecological Processes. *Manual of Environmental Microbiology*, 704–711. https://doi.org/10.1128/9781555815882.ch58

13. Zhang, H., & Zhou, Z. (2018). Recalcitrant carbon controls the magnitude of soil organic matter mineralization in temperate forests of northern China. *Forest Ecosystems*, *5*(1). https://doi.org/10.1186/s40663-018-0137-z

14. Allison, S. D. (2005). Cheaters, diffusion and nutrients constrain decomposition by microbial enzymes in spatially structured environments. *Ecology Letters*, *8*(6), 626–635. https://doi.org/10.1111/j.1461-0248.2005.00756.x

15. Wang, H., Squina, F., Segato, F., Mort, A., Lee, D., Pappan, K., & Prade, R. (2011). High-temperature enzymatic breakdown of cellulose. *Applied and Environmental Microbiology*, *77*(15), 5199–5206. https://doi.org/10.1128/aem.00199-11

16. Naraian, R., & Gautam, R. L. (2017). *Beta-xylosidases*. Beta-Xylosidases - an overview | ScienceDirect Topics. Retrieved April 2, 2023, from https://www.sciencedirect.com/topics/engineering/beta-xylosidases

17. Yanase, H. (2014). *Xylose*. Xylose - an overview | ScienceDirect Topics. Retrieved April 2, 2023, from https://www.sciencedirect.com/topics/agricultural-and-biological-sciences/xylose

18. Song, E. H. (2012). *Chitin*. Chitin - an overview | ScienceDirect Topics. Retrieved April 2, 2023, from https://www.sciencedirect.com/topics/earth-and-planetary-sciences/chitin

19. Bull, H., Murray, P. G., Thomas, D., Fraser , A. M., & Nelson, P. N. (2002). *Acid phosphatases*. Molecular pathology : MP. Retrieved April 2, 2023, from https://pubmed.ncbi.nlm.nih.gov/11950951/

20. Holtan, H., Kamp-Nielsen, L., & Stuanes, A. O. (1988, January 1). *Phosphorus in soil, water and sediment: An overview*. SpringerLink. Retrieved December 9, 2022, from https://link.springer.com/chapter/10.1007/978-94-009-3109-1_3

21. Fox, J. F. (1979). Intermediate-disturbance hypothesis. *Science*, *204*(4399), 1344-1345.

22. Souza, A. F., & Longhi, S. J. (2019, May 27). *Disturbance history mediates climate change effects on subtropical forest biomass and dynamics*. Ecology and evolution. Retrieved April 3, 2023, from https://www.ncbi.nlm.nih.gov/pmc/articles/PMC6662394/

23. Nuñez, H. R., & de Gouvenain, R. C. (2015). Seasonal variation in understory light near a gap edge and its association with conifer seedling survival in a southern New England Forest. *Northeastern Naturalist*, *22*(3), 613–629. https://doi.org/10.1656/045.022.0315

24. Bell, C.W., Fricks, B.E., Rocca, J.D., Steinweg, J.M., McMahon, S.K. and Wallenstein, M.D., 2013. High-throughput fluorometric measurement of potential soil extracellular enzyme activities. *JoVE (Journal of Visualized Experiments)*, (81), p.e50961.

25. United States Department of Agriculture. (n.d.). *Nitrogen in the environment: Mineralization - immobilization*. University of Missouri Extension. Retrieved April 8, 2023, from https://extension.missouri.edu/publications/wq260